Desalination and Water Treatment
www.deswater.com
doi: 10.5004/dwt.2023.29498

292 (2023) 165–175
April

Assessment of the natural zeolite adsorption capacity for the removal of triclosan from the aqueous medium

Beatriz de Souza Gonçalves Proença[a], Rodrigo de Souza Antonio[b], Luís Fernando Cusioli[b], Marcelo Fernandes Vieira[b], Rosângela Bergamasco[b], Angélica Marquetotti Salcedo Vieira[c,*]

[a]*Postgraduate Program in Food Science, Centre of Agrarian Sciences, State University of Maringa, Av. Colombo, 5790, 87020-900, Maringa, Parana, Brazil, Tel.: 55-44-3011-4782, email: beatriz.sgproenca@gmail.com*
[b]*Department of Chemical Engineering, State University of Maringa, Av. Colombo, 5790, 87020-900, Maringa, Parana, Brazil, Tel.: 55-44-3011-4782, emails: z.rodrigo.antonio@gmail.com (R. de Souza Antonio), luiscusioli@gmail.com (L.F. Cusioli), mfvieira2@uem.br (M.F. Vieira), rbergamasco@uem.br (R. Bergamasco)*
[c]*Department of Food Engineering, State University of Maringa, Av. Colombo, 5790, 87020-900, Maringa, Parana, Brazil, Tel.: 55-44-3011-5093, email: amsvieira@uem.br*

Received 10 October 2022; Accepted 23 March 2023

ABSTRACT

The environment has been affected by pollutants originated from production activities, impacting the quality of water. An emerging contaminant found in superficial waters and highly studied is the triclosan (TCS). It is used in personal care products, whose removal is not possible by means of conventional water treatments processes, causing serious problems. Hence, effective removal of this contaminant is required. The adsorption arises as an effective and inexpensive method, where the only main issue is to find low-cost absorbents to make feasible its application. Zeolites are abundant materials with advantageous properties and economically accessible. Therefore, the aim of this study was to use natural zeolites for TCS adsorption from the aqueous medium. Accordingly, the characterization of the adsorbent was carried out as well as the tests to determine the optimal operational parameters. In this sense, the kinetics that better adjusted to data was the pseudo-second-order. The Langmuir isotherm showed the best fit with a maximum capacity of 82.25 mg·g^{-1} at 318 K. Thermodynamic parameters revealed a spontaneous and exothermic process. Regarding the reuse of the adsorbent, it maintained its operational conditions through the five cycles with no loss of efficiency reported. These results show the effectiveness of natural zeolites in the removal of TCS, using small mass of adsorbent which can be reused, being, therefore, an environmentally suitable alternative in water treatment.

Keywords: Natural zeolite; Adsorption; Triclosan; Kinetic study; Isotherm study

1. Introduction

The triclosan ($C_{12}H_7Cl_3O_2$) is an antimicrobial agent used in personal care products such as soaps, toothpaste, shampoo, deodorants, cosmetics and even food packaging. The residual material coming from this contaminant are conducted through the municipal sewage system towards the wastewater treatment plants (WWTP), being often transmitted to the aqueous medium once the triclosan (TCS) is resistant to the degradation processes (e.g., mainly biological) of the water treatment plants. Some recent studies have reported that although TCS has great commercial utility,

* Corresponding author.

it is an emerging contaminant highly toxic to the aquatic organisms such as seaweeds, invertebrates and fishes, even at trace levels ($ng \cdot L^{-1}$). Posteriorly, can lead to damage to mammals through the food chain [1–4].

The damages can range from allergies, developmental and reproductive impairments, immunological system weakening, carcinogenicity, endocrine disorders, among others. Considering these impacts, in December 2017, the Food and Drug Administration agency from the USA decided to suspend the commercialization of triclosan-based soaps without medical prescription, considering that it is "not recognized as safe and effective". In addition, the European Commission settled the reproval of the TCS use in personal care biocides products. In order to avoid the TCS damage to the aquatic environment, it is convenient to seek for selective and effective adsorbents for the removal of TCS [1–4].

According to Lu et al. [5], the harmful effect of TCS was mainly observed throughout the COVID-19 pandemic, where various antibacterial hand sanitizers were discarded, affecting both the environment and human health.

Several studies have reported the TCS removal, where different adsorbents have been used. Simple walled carbon nanotubes were used by González-Fernández et al. [6] while Behera et al. [7] used charcoal-based activated carbon, kaolinite and montmorillonite. Triwiswara et al. [8] used char derived from palm kernel shell, while kenaf-derived biochar were used by Cho et al. [9]. Other authors also used low-cost adsorbents to remove triclosan, Cho et al. [10] used biochar derived from seed shell of *Aesculus turbinata* and Kang et al. [11] used food waste biochar. Some studies also applied low-cost adsorbents, but to remove different contaminants such as Cr(VI) and NH^{4+} adsorption using greensand (glauconite) by Naghipour et al. [12] and diclofenac removal from aqueous solution by activated carbon derived from pine tree Naghipour et al. [13]. Finally, Hu et al. [14] studied the ability of purified multi-walled carbon nanotubes to adsorb diclofenac and triclosan in aqueous solutions.

There are several techniques for contaminant removal such as adsorption, biological systems, chemical precipitation, ultrafiltration, processes with membranes, ionic change, reverse osmose and electrochemical processes. However, the majority of these aforementioned techniques present disadvantages as low selectivity, high cost, low remotion rates, which make the application of these techniques unfeasible [15]. Mohapatra and Kirpalani [16] observe that treatments are applied according to effluent quality requirements, besides depending on the final destination.

Among the techniques addressed, the adsorption stands out as an advantageous process due to its simplicity, low-cost and ease of implementation [17]. Moreover, it is a promising technique with a high efficiency rate [18]. In addition, it has a low energy expenditure and great adaptability with regard to the materials used as adsorbents [19]. Mohapatra and Kirpalani [16] point out that the adsorption can be done using granular activated charcoal, zeolites or other clay materials. Du et al. [20], however, reported the necessity of developing effective and economically feasible adsorbents for water purification.

Techniques that use natural adsorbents as zeolites have been shown to be effective in removing contaminants considering the technological accessibility and economic feasibility [15]. Zeolites are materials composed of hydrated crystalline aluminosilicates from alkaline and alkaline earth cations, with a tri-dimensional connected pore structure. They are well known as "molecular sieves" due to their microporous structure. There is plenty of zeolites that have been described so far. Nonetheless, the common types of zeolites are referred as clinoptilolite [21].

The zeolites are widely used by reason of their ionic, adsorptive and catalytic change properties as well as their structural diversity. There is increasingly demand over the last decades in the utilization of natural zeolite (NZ), given that they are inexpensive, easily available and eco-friendly [22,23].

Considering that the TCS is used in personal care products, as well as in various antibacterial hand sanitizers, is easily found as an emerging contaminant, is difficult to remove using conventional techniques, and its highly hazardous chlorinated subproducts, the aim of the present study was to use the clinoptilolite-type NZ for the TCS removal from the aqueous medium applying the batch adsorption technique.

2. Materials and methods

2.1. Materials and reagents

The natural zeolite used in the experiments was donated by the company Celta Brazil, and the reagents included the triclosan ($C_{12}H_7Cl_3O_2$) from Sigma-Aldrich (99% of purity), ethyl alcohol (CH_3CH_2OH) from the Synth brand (99.5% purity), and methyl alcohol (CH_3OH) from the Fmaia brand (99.8% purity), as well as the salts used in the ions interference study, sodium chloride (NaCl) from Synth (99% purity), calcium chloride ($CaCl_2$) from Anidrol (99% purity), magnesium chloride ($MgCl_2$) from Synth (99% purity) and potassium chloride (KCl) from Synth (99% purity). The solvents applied in the desorption process were methyl alcohol, ethyl alcohol (details already mentioned) as well hydrochloric acid (HCl) from nuclear and sodium hydroxide (NaOH) from Anidrol N in capital letters, as it is the loam of the reagent.

2.2. Characterization

With the aim of characterizing the NZ used as adsorbent, instrumental techniques such as the scanning electron microscopy coupled with energy-dispersive X-ray spectroscopy (SEM/EDS), transmission electron microscopy (TEM), Fourier-transform infrared spectroscopy (FTIR), X-ray diffraction (XRD), X-ray fluorescence (XRF) and zeta potential, were applied to assess the morphology, structure, and elementary composition of clinoptilolite-type NZ.

The analyses by SEM/EDS to verify the NZ morphology was performed using an electronic microscope Quanta 250-FEG (FEI Company) equipped with the EDS-type chemical analysis system (Oxiford). The TEM analysis was conducted by fixing the sample in copper grids, analyzing it through a microscope (JOEL JEM-1400) of 120 kV. Both microscopy analyses were performed at the Research Support Center Complex (COMCAP – UEM). The FTIR was executed with spectra collected between 4,000 and 500 cm^{-1}, with resolution of 2 cm^{-1} and 21 scans/min^{-1}, using a spectrophotometer

Shimadzu model IR PRESTIGE-21, from the Multiuser Central Spectroscopy Laboratory (PROPPG – UEL), for the assessment of the zeolite functional groups. The XRD analysis was carried out using a diffractometer from PANalytical, model Empyrean. The samples were exposed to X-rays contemplating the angles from 5° to 80° in 2Θ with potency of 45 kV and 40 mA, using tubes with cooper anode. The determination of amorphous content was performed by the internal standard method. In this case we used the anatase (TiO_2), and the data obtained were analyzed using the HighScore v 3.0 software to build the diffractogram. This procedure, as well as the XRF, were conducted by the Celta Brasil company, in accordance with the NBR 12677/2014. A particle analyzer (DelsaTMNanoC, Beckham Coulter) was used to define the adsorbent zeta potential, applying a solution composed of 0.03 g of biosorbent and 30 mL of deionized water, adjusting and varying the pH in the range of 2 to 12.

2.3. Triclosan synthetic solution preparation

The TCS solutions were prepared with concentrations that ranged from 10 to 50 mg·L^{-1}, which were applied in batch adsorption process. A standard of 99% purity was defined, wherein the dilution was performed in 30% ethyl alcohol solution and deionized water, due to TCS low solubility in pure water. The solutions were homogenized with the aid of a magnetic stirrer to assure a complete dissolution. Sequentially, the concentration interpretation was performed using a spectrophotometer UV-VIS (HACH DR 5000) in a wavelength of 280 nm.

2.4. Adsorption experiments

Initially, the zeolites were washed with deionized water for the removal of impurities. Thereafter, it underwent a drying process in a heater with air circulation at 343 K. It was sifted to standardize the adsorbent granulometry, which established a particle diameter range of 600–425 μm. The preliminary experiments were performed in batches, fixing the following parameters: 24 h, temperature at 298 K and orbital stirrer rotation at 150 rpm considered ideal according to Khori et al. [24], and 30 mL of solution with a contaminant concentration of 20 mg·L^{-1}, in which the adsorbent mass and solution pH were determined after studying the effect of these parameters. The adsorption capacity q_e (mg·g^{-1}) of the studied contaminant by the adsorbent is calculated using Eq. (1):

$$q_e = \frac{(C_0 - C)V}{m} \tag{1}$$

where C_0 and C are the initial and final drug concentration (mg·L^{-1}), V is the solution volume (L), and m (g) is the adsorbent mass.

2.5. Adsorbent mass and pH influence

Experiments were carried out to analyze the pH and adsorbent mass influence on the adsorptive process, in order to define the optimal conditions regarding these parameters and further application in the kinetics and isotherm experiments. Accordingly, the aforementioned parameters were maintained, varying only the adsorbent mass (e.g., 0.01, 0.02, 0.03, 0.04 and 0.05 g). Posteriorly, the adsorption capacity (q_e) was calculated with the aim of defining the best adsorbent mass. After determining the optimal adsorbent mass value, the pH influence was tested. The parameters were also maintained for all tests and the pH was tested at 4, 7, and 10, calculating hence the q_e to establish the ideal pH for the next steps.

2.6. Adsorption kinetic

Khori et al. [24] reported that the reaction kinetics is essential to define the adsorption rate of the adsorbate during the adsorption process. Optimized parameters of mass and pH were used, keeping the other conditions fixed. The sample aliquots were collected in previously defined times. In sequence, the samples were filtered with the aid of a cellulose acetate membrane of 0.45 mm. The final concentration reading was performed using a spectrophotometer UV-VIS to calculate the adsorption capacity. The tests were performed in duplicate. The kinetics results were fitted to the pseudo-first-order model by Lagergren [25] and the pseudo-second-order model by Ho and McKay [26], presented in Eqs. (2) and (3), respectively.

$$q_t = q_e\left[1 - \exp\left(-k_f t\right)\right] \text{ [25]} \tag{2}$$

where q_t (mg·g^{-1}) is the quantity of TCS adsorbed in the time t (min), q_e (mg·g^{-1}) is the quantity of TCS adsorbed in the balance, and k_f is the constant adsorption rate of the pseudo-first-order model.

$$q_t = \frac{k_s q_e^2 t}{1 + q_e k_s t} \text{ [26]} \tag{3}$$

where k_S (g·mg^{-1}·min^{-1}) is the constant adsorption rate of the pseudo-second-order model.

2.7. Adsorption isotherm and thermodynamic parameters

The adsorption isotherms were determined using three different temperatures (298, 308 and 318 K), ranging the TCS concentration from 10 to 50 mg·L^{-1} in a solution of 30 mL, 150 rpm rotation, ideal pH and mass, and the balance time settled by kinetics. After this process, the samples were filtered, and the final concentration reading was taken to determine the adsorption capacity, as well as applying the classic adsorption isotherm model from Freundlich (1906) and the Langmuir (1918). These models are described in the Eqs. (4) and (5), respectively. Model adjustments allowed defining the constants involved in the adsorption process, wherein the model that best fitted the data provides a constant (K_F or K_L) that server as basis for predicting the system behavior, being also applied to calculate thermodynamic parameters such as enthalpy (ΔH), entropy (ΔS), balance constant (K_C) and Gibbs free energy (ΔG).

$$q_e = K_F C_e^{1/n} \tag{4}$$

where K_F is the adsorption capacity constant according to the Freundlich, 1/n demonstrates the existence of affinity between the adsorbent and adsorbate, whereas if the value is lower than 1, the adsorption is favorable.

$$q_e = \frac{q_{\max} K_L C_e}{1 + K_L C_e} \tag{5}$$

where K_L is the adsorption capacity constant according to Langmuir model and $q_{\max}$ is the maximum adsorption capacity (mg·g^{-1}).

Regarding thermodynamic parameters, the Gibbs free energy (ΔG) was calculated according to Eq. (6):

$$\Delta G = -RT \ln K_c \text{ [28]} \tag{6}$$

where R is the universal gas constant (kJ·mol^{-1}·K^{-1}), T is the temperature (K), K_C is an equilibrium constant and ΔG is the Gibbs free energy (kJ·mol^{-1}).

The rearranged equation of van't Hoff was used to calculate enthalpy (ΔH) and entropy (ΔS), according to Eq. (7):

$$\ln K_c = -\frac{\Delta H}{R}\frac{1}{T} + \frac{\Delta S}{R} \text{ [28]} \tag{7}$$

where R is the universal gas constant (kJ·mol^{-1}·K^{-1}), T is the temperature (K), K_C is an equilibrium constant, ΔH is the enthalpy (kJ·mol^{-1}) and ΔS is the entropy (kJ·mol^{-1}·K^{-1}).

2.8. Ions competition study

The aim of this stage of the study was to verify the interference of the trivial salts, as well as their respective dissociated ions in the TCS adsorption capacity. Therefore, sodium chloride (NaCl), calcium chloride ($CaCl_2$), magnesium chloride ($MgCl_2$) and potassium chloride (KCl) in molar proportions of dissociated ions from 0.1 to 0.3 M were used in the adsorptive process. The contact time stipulated for this stage was 24 h, at 298 K, using an orbital shaker (Tecnal, TE 4200), and the other optimal parameters found throughout the research. The adsorption capacity was measured after the end of the contact time in the interest of predicting the ions interference in the process.

2.9. Adsorbent reuse and desorption

In this phase, the aim was to determine the likely reutilization of the adsorbent, considering that the procedure occurred in two ways. Firstly, the performed adsorption process was the one previously mentioned, using the balance time after kinetics. Posteriorly, the desorption stage was performed, where solvents were applied to remove the contaminant from the active sites of the adsorbent. The solvents applied in the desorption process were methyl alcohol 100% and 50%, ethyl alcohol 100% and 50%, HCl 0.1 M, and NaOH 0.1 M. The solvent that presented the best result was indeed applied in the reuse study. After choosing the best solvent, 60 mL of this solvent was used to desorb the TCS from the zeolite pores. Considering the mass lost over the cycles, it was used twice the mass and volume in relation to the other experiments. Thus, 0.02 g of saturated and dried zeolite were added with the solvent in the desorption solution and placed in the orbital shaker at 150 rpm in the equilibrium time. The solution was then filtered, and the adsorbent was dried in a heater to be applied in the next adsorption/desorption cycle. Finally, the adsorbed and desorbed quantities were calculated by means of Eqs. (1) and (8), respectively.

$$q_{\text{ed}} = \frac{\left(C_{\text{ed}} V_r\right)}{m_s} \tag{8}$$

where q_{ed} (mg·g^{-1}) is the quantity of triclosan desorbed in the balance, C_{ed} is the concentration of triclosan desorbed in the fluid phase (mg·L^{-1}), V_r is the desorption solution volume (L), and m_s is the saturated adsorbent mass used (g).

3. Results

3.1. Characterization

Regarding the characterization results, Fig. 1 presents the morphology obtained by the SEM, in a magnification of 5,000×, where it can be superficially observed the presence of pores on the zeolites with regions where the components are retained after the adsorption process. The pores did not present a regular shape, however, it can be observed the presence of many distinct pores.

The conformation presented in the SEM image by Lei et al. [27] was similar to the one found in the current study. The authors described it as a crystal with a tabular tendency, a flat shape similar to overlapping coverslips, quite usual in clinoptilolite.

Fig. 2 corresponds to the EDS, where it can be verified the superficial composition of the zeolite. As expected, it was possible to observe the presence of silicon, aluminum and oxygen, which are in fact the molecules present in the material structure that form the tetrahedrons according to the literature. The copper traces observed can be due to

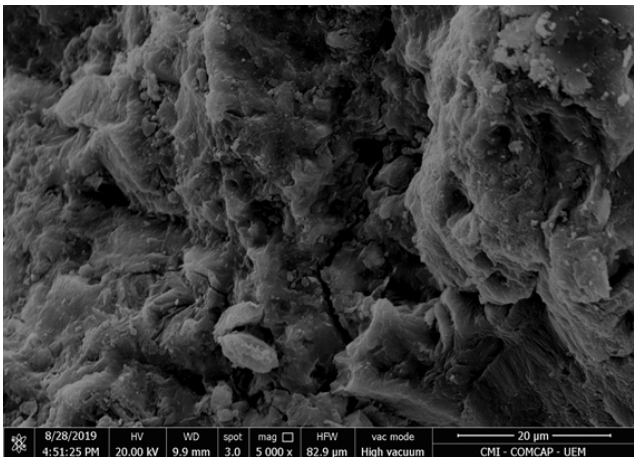

Fig. 1. Natural zeolites scanning electron microscopy with image zoom of 5,000×.

the sample metallization. These traces had a low intensity, precluding its quantification. As reported by Ramos et al. [29], zeolites are materials composed of hydrated crystalline aluminosilicates of alkali cations and alkali earth cations, structured in stiff and tri-dimensional crystalline networks formed by SiO_4 and AlO_4 tetrahedral and TO_4 variations (T = Si, Al, B, Ge, Fe, P, Co, etc.), linked by oxygen atoms.

The XRD was applied to identify the crystalline structure of the adsorbent. Fig. 3 expresses the diffractogram that represents the NZ structure.

According to the diffractogram, it is possible to verify the presence of complex molecules as well as the amorphous region of the NZ. The complex region is composed of 68.57% of clinoptilolite, 11.66% of mordenite, 17.29% of muscovite, and 2.47% of amorphous region. Based on Tisler et al. [30], the clinoptilolite (Si:Al > 4) belongs to the heulandite group and it is the main component of the NZ. Its structure is formed of a porous 2D system with two types of eight-members rings and one ten-member ring. The channels of these rings are occupied by exchangeable cations, ions and water molecules [18].

Fig. 4 represents the zeolite internal morphology, obtained through TEM. According to the image, the inside of the sample is composed of complex molecules already defined in the XRD as clinoptilolite, modernite and amorphous regions, the latter representing 2.47% of the sample.

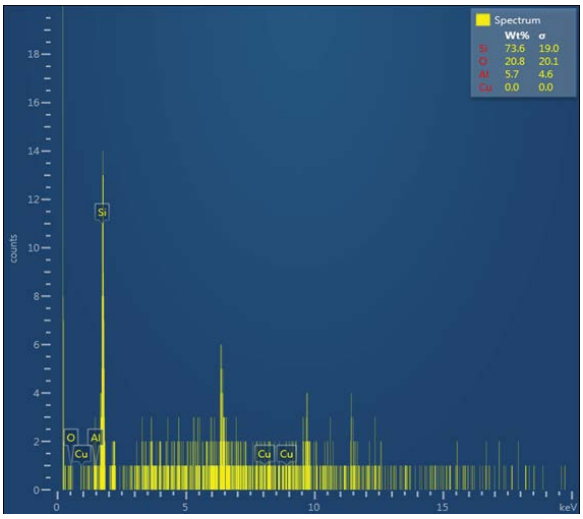

Fig. 2. Scanning electron microscopy coupled with energy-dispersive X-ray spectroscopy to verify the superficial composition of the zeolite structure.

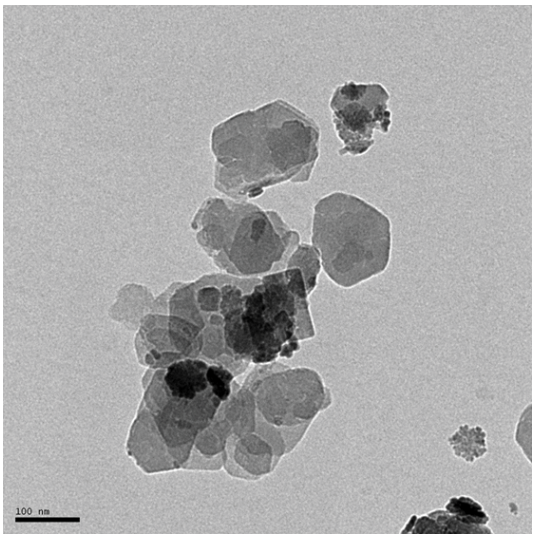

Fig. 4. Natural zeolite internal structure showed by means of transmission electron microscopy.

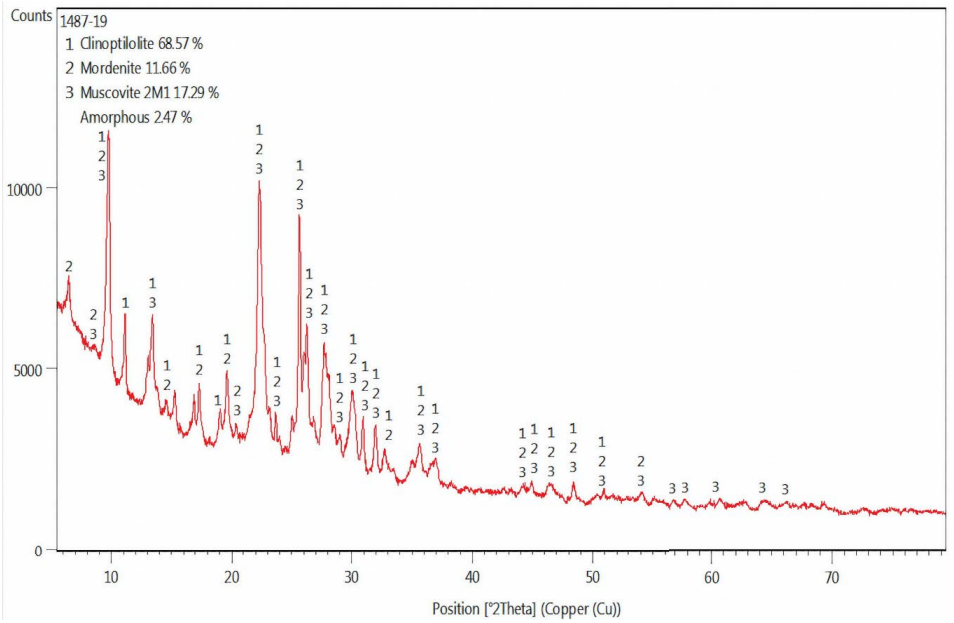

Fig. 3. Diffractogram of the crystalline structure of the natural zeolite obtained by means of X-ray diffraction.

With the aim of matching the morphology presented in the SEM/EDS and the components present in the NZ, it was submitted to the XRF. As can be seen in Table 1, the presence of mainly oxygen-bond silicon and aluminum confirms the outcomes verified in the SEM/EDS.

Lei et al. [27] mentioned in their study that the main chemical composition of NZ based on the XRF analysis were SiO_2 (69.39%), Al_2O_3 (12.72%), Na_2O_3 (2.70%), CaO (2.61%), MgO (0.33%), K_2O (1.44%), and Fe_2O_3 (0.87%). These values are similar to those from this study, as can be seen in Table 1.

The main adsorbent functional groups determination, collected using the FTIR technique, is expressed in Fig. 5.

The FTIR is one of the most important techniques to identify and determine the functional groups of the adsorbents that will exert a direct influence in the adsorption process [24].

Lei et al. [27] stated that in the spectrum referred to the FTIR, the most common band positions were 3,622; 3,421 cm^{-1} (the –OH vibration stretching), 1,044 cm^{-1} (the Si–O–Si stretching vibration in the silicon), and the sorption at 1,638 cm^{-1} in the spectrum was due to the water directly coordinated to the exchangeable cations of the zeolite. These peaks also appeared in the FTIR performed to the studied material, despite presenting differences in the mineralogical phase, as already compared in the XRD. The authors reported the adsorbent spectrum in the region of 4,000–400 cm^{-1}. Meanwhile, in this study, the spectrum was registered in the region of 4,000–500 cm^{-1}.

According to Mantovani et al. [31], low vibrations observed in the wavelength 534 cm^{-1} correspond to the Ca–O. In the XRF presented in Table 1, it was possible to verify the presence of a small quantity of CaO in the zeolite structure. Regarding the band of 3,707–3,633 cm^{-1}, it indicates hydrogen bonds as reported by Araújo et al. [32].

Fig. 6 presents data concerning the adsorbent zeta potential. Accordingly, it is possible to observe that all the potential values were negative, regardless of the pH used. Therefore, it is interesting to use contaminants with positive charges in order to facilitate the ionic change in the adsorption process.

As observed in the zeta potential of the adsorbent, it presents only negative charges, and these charges increase negatively with an increase in the pH. Thus, the adsorption needs to be well controlled, once Behera et al. [7] stated that the TCS can exist in both neutral and ionized form, depending on the solution pH. Hence, there is an electrostatic repulsion between the negatively charged surface of the zeolite which is similar to the natural and the TCS species negatively charged, disfavoring the TCS adsorption with an increase in the pH.

These characterizations are essential to determine the chemical elements, functional groups and other adsorbent information, and useful to predict the mechanism of the adsorptive process.

Table 1
Structural determination by X-ray fluorescence

Chemical elements	Results (%)	Chemical elements	Results (%)
Ignition loss	9.14	Na_2O	1.61
SiO_2	71.04	K_2O	1.67
Al_2O_3	11.57	MnO	<0.01
Fe_2O_3	1.76	P_2O_5	<0.01
MgO	0.72	ZnO	<0.01
CaO	2.41	CuO	<0.01
TiO_2	0.23	Ag_2O	<0.01

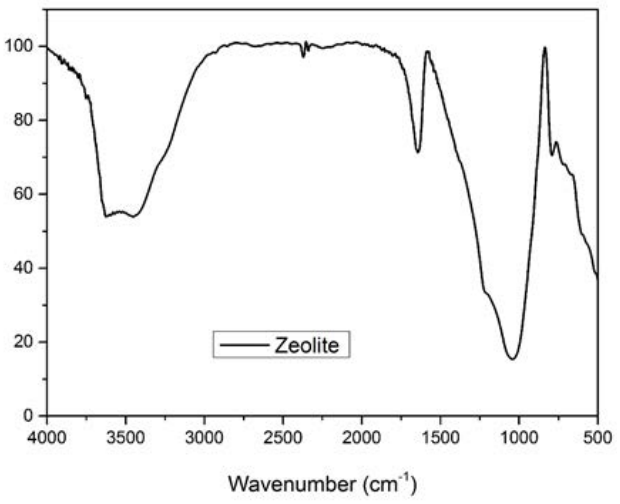

Fig. 5. Structural determination of natural zeolite by the Fourier-transform infrared spectroscopy.

3.2. Study of the mass and pH

Regarding the adsorption experiments, the adsorbent mass parameters and the pH of the solution for the adsorptive process were verified. Fig. 7 shows the results of the adsorbent mass variance.

In line with the data obtained from the study of the mass influence in the adsorption process, it was possible to settle an optimal value in relation to this parameter. A mass of 0.01 g was used for the posterior tests, since there

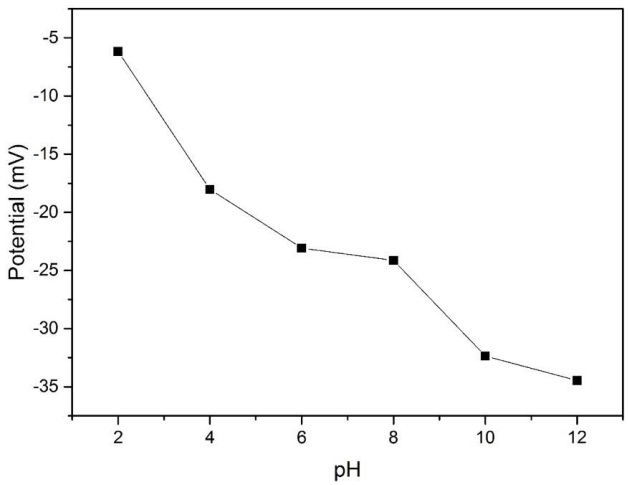

Fig. 6. Zeta potential of the adsorbent.

is a high remotion as well as adsorptive capacity. Lei et al. [27] also used 0.01 g of zeolite in their study; however with a concentration of 40 mg·L^{-1} and 10 mL of TCS solution. Nevertheless, the zeolites used by the authors were modified in the interest of increasing the efficiency.

Khori et al. [24] also used 0.01 g of adsorbent (e.g., coconut pulp residual-derived activated charcoal) in their study, with 50 mL of solution and only 5 mg·L^{-1} of TCS. Nonetheless, the authors mentioned that the utilization of a higher mass could cause an overlap of the adsorption sites by virtue of a clustering of the adsorbent particles, diminishing the number of active sites for adsorption. Despite diminishing the adsorption capacity due to the concentration gradient between the adsorbate concentration in the solution and the adsorbent surface, it also reduces the quantity of the adsorbed contaminant per unity of adsorbent mass.

With a fixed mass, the pH was modified to verify its influence. The results demonstrated an adsorption capacity of 17.49, 17.69 and 15.36 for the pH 4, 7 and 10, respectively. Therefore, pH 7 was settled for the further studies, on the grounds that the results were similar for the acid, neutral and basic pH. Then, the natural pH was used to facilitates the tests. González-Fernández et al. [6] also used pH 7 to remove TCS with simple walled carbon nanotubes (SWCNTs). The results of the authors showed a maximum adsorption capacity of TCS at pH 7 of 30.3 mg·g^{-1}. Behera et al. [7] studied the sorption of TCS on three sorbents, viz., activated carbon, kaolinite and montmorillonite, and found a maximum adsorption capacity of 30, 6.4 and 19.3 mg·g^{-1} for activated carbon, kaolinite and montmorillonite, respectively. While in this work, the maximum adsorption capacity of TCS at pH 7 was 17.69 mg·g^{-1}. Behera et al. [7] mentioned that at acidic pH, the electrostatic interaction is unlikely to occur as a consequence of the neutral form of the TCS in the solution. The hydrophobicity of the TCS decreases in basic pH. This decrease in hydrophobicity with increasing pH results in a decrease in hydrophobic interactions.

Thus, it is possible to infer that the chosen pH was the ideal one for the related process, given that it is not low enough to cause repulsion of charges and also not high enough to promote a decrease in the hydrophobic interactions, hampering the adsorption.

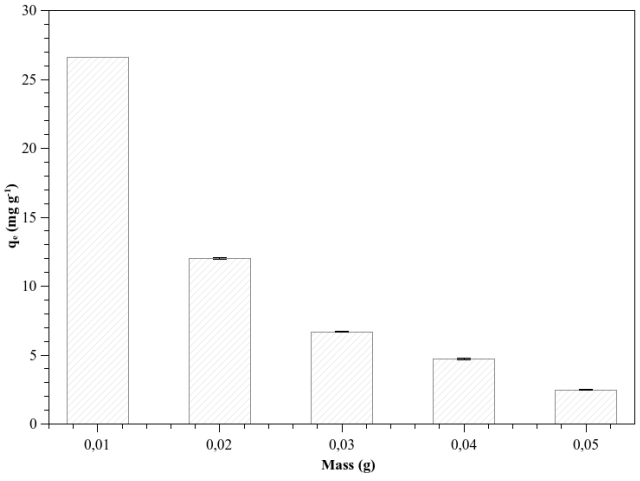

Fig. 7. Influence of the adsorbent mass in the adsorption process.

3.3. Adsorption kinetics

In line with the previous adsorption studies already mentioned, the kinetics study was performed, being the pseudo-first-order and pseudo-second-order models posteriorly adjusted to the experimental data. Fig. 8 presents the adsorption results and kinetics adjustments.

It was possible to observe in Fig. 8 and Table 2 that the experimental data best fitted the pseudo-second-order model, considering the R^2 of 0.991, showing a good adjustment. Moreover, the c^2 (reduced chi-square or weighted mean squared deviation) also assess the quality of the adjustment. In this case, the pseudo-second-order model (c^2 = 0.679) presented a better adjustment in comparison to the pseudo-first-order (c^2 = 1.042), assuring higher deviations for the pseudo-first-order. Finally, the q_e for the pseudo-second-order model was slightly higher. According to these findings, the better adjustment to the pseudo-second-order is evidenced. This is in agreement with the findings reported by Kaur et al. [33], Hu et al. [14] and Cho et al. [9] which have also adjusted their data to the pseudo-second-order model. González-Fernández et al. [6], however, used first order kinetic model and the diffusional model. Furthermore,

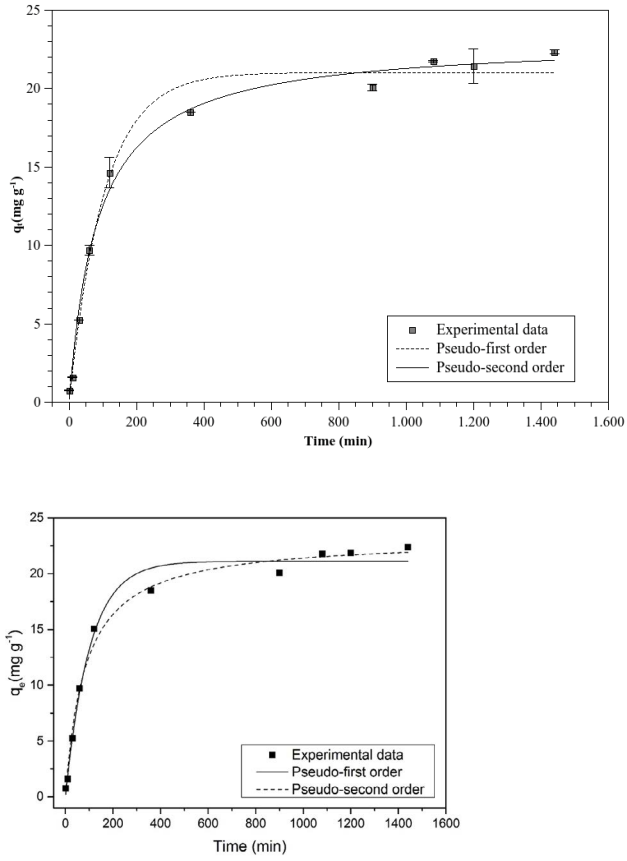

Fig. 8. Adsorption kinetics study and experimental data adjustments to the pseudo-first-order and pseudo-second-order kinetic models.

Lei et al. [27] reported that the similar-to-natural zeolite TCS adsorption occurs in the monolayer. According to da Silva et al. [34], the adsorption rate in the pseudo-second-order model is dependent on the quantity of chemical specie adsorbed in the adsorbate surface as well as the quantity adsorbed in the balance state.

3.4. Adsorption isotherm

The experiment related to the adsorption isotherm was performed, adjusting posteriorly the data to the Freundlich and Langmuir traditional models, as can be observed in Fig. 9.

Concerning Fig. 9, the main highlight of the isotherm study was the possibility of a great triclosan removal with a small quantity of adsorbent, which led to a high q_e. Of note, the q_e increased with an increase in the concentration for all the tested temperatures, with a greater increase at 318 K. Table 3 relates the mathematical models for isotherms used to describe the adsorptive process. Interestingly, the two models applied represent the isotherm. Nevertheless, the Langmuir model is more suitable to the current data. According to Triwiswara et al. [35], this indicates that triclosan was adsorbed on a monolayer. Moreover, it was possible to observe that at a temperature of 318 K, applying the Langmuir model, the maximum adsorption capacity was 82.246 mg·g^{-1}, which is very close to the maximum capacity of 88.854 found by Triwiswara et al. [35] that evaluated char derived from palm kernel shell (PKS-char) as an adsorbent for the removal of triclosan. Meanwhile, Cho et al. [9] found a maximum triclosan adsorption capacity of 77.4 mg/g, also obtained from the Langmuir model with a high correlation coefficient, using kenaf-derived biochar. Thus, it is convenient to adjust the Langmuir model and use the obtained Langmuir constant to calculate the subsequent thermodynamic parameters. Hu et al. [14] also founded that the two models applied represent the isotherm, but the Freundlich model fitted better, while in this case the Langmuir model fitted better to the data.

According to Nascimento et al. [36], when analyzing the isotherms, relevant information about the adsorption process can be obtained.

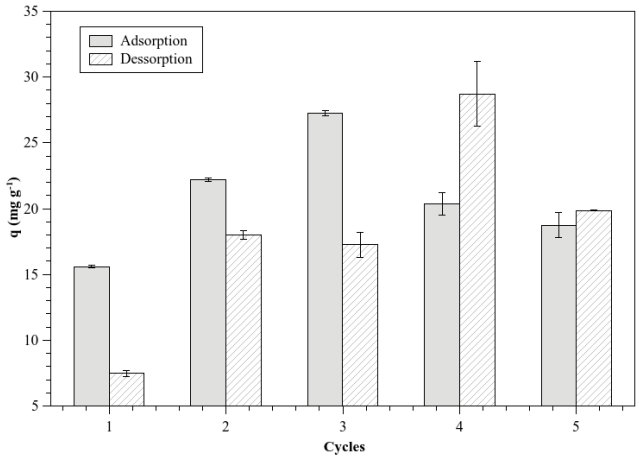

Fig. 9. Adsorbent reuse cycles.

Table 2
Parameters of the models applied to the kinetics

Models	Parameters	Values
Pseudo-first-order	q_e (mg·g^{-1})	21.118
	k_f (min^{-1})	0.009
	R^2	0.986
	χ^2	1.042
Pseudo-second-order	q_e (mg·g^{-1})	23.182
	k_S (g·mg^{-1}·min^{-1})	5.163 × 10^{-4}
	R^2	0.991
	χ^2	0.679

3.5. Thermodynamic parameters

Table 4 details the thermodynamic parameters obtained in the adsorptive process.

Accordingly, Lei et al. [27], who studied the removal of TCS using organo-zeolites (OZs) prepared by loading cetylpyridinium bromide (CPB), found a ΔG of –28.35 (kJ·mol^{-1}), while a value of –25.19 (kJ·mol^{-1}) was found in the current study. The same authors found a ΔS of 0.06 (kJ·mol^{-1}), while a value of 0.19 kJ·mol^{-1}·K^{-1} was reported in this study.

The ΔG values were all negative, which means that the process occurs spontaneously. According to Vimonses et al. [37], in general, the free energy for a physisorption is in the range of 20 to 0 kJ·mol^{-1}. Meanwhile, the free energy for a chemosorption varies between 80 and 400 kJ·mol^{-1}. The ΔG values were closer to the range described as physisorption. Lei et al. [27] suggested that the TCS adsorption was essentially a hydrophobic physisorption process, including other adsorption process, as the anion exchange.

Hu et al. [14] studied the adsorption of diclofenac and triclosan by purified multi-walled carbon nanotubes and

Table 3
Parameters of the models applied to the isotherm

Models	Parameters	298 K	308 K	318 K
Freundlich	K_F (mg·g^{-1})(mg·L^{-1})^{nF}	10.075	10.728	24.008
	n_F (L·mg^{-1})	2.400	2.119	2.999
	R^2	0.968	0.970	0.929
Langmuir	K_L (L·mg^{-1})	0.090	0.076	0.204
	q_{max} (mg·g^{-1})	56.463	75.953	82.246
	R^2	0.995	0.992	0.993

Table 4
Thermodynamic parameters

T (K)	ΔG (kJ·mol^{-1})	ΔH (kJ·mol^{-1})	ΔS (kJ·mol^{-1}·K^{-1})
298	–25.19		
308	–25.60	–31.82	0.19
318	–29.05		

found a enthalpy value of –27.01 kJ·mol^{-1}, while in this work a value of –31.82 kJ·mol^{-1} was observed.

The ΔH value indicates whether the process is endothermic or exothermic. Thus, a negative ΔH value indicates an exothermic process. The ΔS value indicates that the system is in a natural process of disorder, while the liquid and solid molecules that compose the adsorptive system are disorganized and randomly disposed. Kang et al. [11] who studied the adsorption mechanism of food waste biochar for triclosan removal, also stated in their studies spontaneous and exothermic processes.

3.6. Ion competition study

Regarding the ion competition study, the results are demonstrated in Table 5.

The ionic force study allowed us to observe that the majority of the studied ions did not influence the adsorptive process, considering the low final concentration reported after the process. The ion that interfered in the adsorption was the Ca, especially in the concentration of 0.3 M, in which a competitive adsorption might have occurred, where the Ca ions competed with the TCS for the same adsorbent active site. Blanchard et al. [38] affirms that the NZ has low selectivity in relation to calcium absorption. Contrariwise, the Mg favored the adsorption, especially in the concentration of 0.3 M, having in mind that the residual content was low, which implies an effective adsorption. Karthik and Philip [39] used some adsorbents to remove diclofenac, carbamazepine, and ibuprofen. They observed an increase in the removal of diclofenac and ibuprofen in the presence of cations using brickbats and blast furnace slag as adsorbents. According to these authors, the cations could form a bridge between the anionic compounds and the negatively charged surface of the adsorbent. This may lead to a slight increase in pollutant removal.

3.7. Adsorbent reuse study

Following the desorption study, it was possible to predict the reuse cycle quantity that the adsorbate is able to perform without significantly losing efficiency. Some solvents were tested to verify the best performance in the desorption study. Basic and acid solutions were used in a concentration of 0.1 M altogether with 100% and 50% methyl and ethyl alcohol. From these, the best solvent for the desorption process was the 100% methyl alcohol. Considering that the NZ can remove almost all the TCS in the adsorption and desorption process, the 100% methyl alcohol was the solvent that could better move the TCS that was retained in the zeolite pores to the liquid medium, therefore, it was the one used in the reuse tests.

According to the desorption studies, it can be observed in Fig. 9 that using a TCS solution with a 15 mg·L^{-1} concentration in the adsorption and 100% methyl alcohol for desorption, the adsorbate maintained its efficiency up to 5 cycles.

It is notable the stable efficiency of the NZ after 5 adsorption/desorption cycles. This is a relevant factor because, although it is an abundant and low-cost material that would not need to be reused, it still has the advantage of being able to be reused.

The regularity of the adsorption values obtained in all cycles needs to be highlighted. Still, it was possible to observe that the adsorption/desorption capacity increased until the third cycle. The oscillation in adsorption/desorption values it might be due to some variation in the experimental parameters or even a natural zeolite behavior.

A plausible explanation for this increase until the third cycle and subsequent decline would be that the adsorbate is serving as an active site until saturation. That is, TCS comes into contact with NZ, binds to its active site and after desorption, the triclosan that was more strongly bound to the zeolite and was not desorbed, serves as an active site for a new TCS molecule until saturation occurs (from the third cycle onwards), making the adsorptive capacity decrease.

The data obtained for reuse are of substantial importance in the study. Kaur et al. [33] used commercially available activated charcoal for TCS removal and observed that regarding the reuse data, the efficiency of the 1st, 2nd and 3rd regeneration was 92.8%, 86.3%, and 75.2%, respectively.

Although this reuse stage is used to predict the potential reutilization of the adsorbent, the outcomes might also indicate, by more than one factor, that the adsorption was conducted via physisorption. Reck et al. [40] states that an adsorption with weak and reversible interactions are features of a physisorption, and the solvent capable of removing the contaminant from the pores many times over the adsorption/desorption cycle was found in this system, due to the typical physisorption interactions.

Table 5
Effect of the ionic force in the adsorption process

Adsorptive capacity without the presence of ions (mg·g^{-1})	Ions tested concentration	Adsorptive capacity in the presence of the ion (mg·g^{-1})
22.53	$NaCl_2$-0.1 M	25.77 ± 0.127
	$NaCl_2$-0.3 M	28.60 ± 0.191
	$CaCl_2$-0.1 M	21.55 ± 0.021
	$CaCl_2$-0.3 M	0.99 ± 0.085
	$MgCl_2$-0.1 M	28.81 ± 0.615
	$MgCl_2$-0.3 M	28.00 ± 0.170
	KCl-0.1 M	23.73 ± 0.636
	KCl-0.3 M	32.62 ± 0.064

Lastly, the findings were satisfactory, considering that according to Li et al. [41], it is hard to keep coherence in the data since the crystallinity and purity of the natural clinoptilolite varies according to the sample.

3.8. Study limitation and recommendations for future work

Unfortunately, we do not have adequate means to apply a temperature above 318 K, which was the temperature that presented the best results in terms of adsorptive capacity. It would be interesting to carry out a future study applying temperatures higher than those presented in this one. In addition, the batch operating system was used, it would also be important to analyze the behavior of contaminant removal in a continuous system.

The purpose of the work was to use natural zeolite, minimizing costs. However, some modifications could contribute positively to the removal of the contaminant. Whether a chemical or thermal modification, without greatly increasing costs, may add value to the adsorbent. Finally, the standardization of the sample and working conditions are essential when working with natural material in order to replicate the results.

4. Conclusions

The use and posterior deposition of a emerging contaminant such as TCS is worrisome, considering its resistance to treatments, the damage to the aquatic environment, and the human health, by means of the food chain. Thus, the study had as aim the removal of TCS from the aquatic medium via adsorption, applying a natural and abundant material, which is the zeolite. From the outcomes presented, it was possible to observe that the analyses of characterization were useful in the confirmation of the compounds present in the NZ structure, as well as the composition in terms of mineralogical phase, functional groups, among others. Regarding the adsorptive process, the results revealed that the NZ are highly effective as regards the triclosan removal, allowing the removal of the contaminant with a small adsorbent mass. In the kinetic study, the model that better adjusted to the experimental data was the pseudo-second-order, in a balance of 1,080 min with a maximum adsorption capacity of 21.75 $mg \cdot g^{-1}$. Moreover, the NZ was considered selective, once from the ions tested, only one interfered in the adsorption process. The remaining ions did not compete with the TCS for the active sites. Despite being a natural and abundant material, which would not necessarily need to be reused as it was employed *in natura* without chemical or structural changes, the material was reused for five cycles without loss of efficiency.

Declaration of competing interest

None.

Acknowledgements

The authors thank the Celta Brasil company for the partnership, the Research Support Center Complex (COMCAP – UEM), and the Multiuser Central Spectroscopy Laboratory (PROPPG – UEL) by the technological support. The authors also thank the financial support granted by the Coordination for the Improvement of Higher Education Personnel (CAPES) Financing Coode 001, and National Council for Scientific and Technological Development (406200/2021-1 CNPq).

References

[1] Y.C. Lu, J.H. Mao, W. Zhang, C. Wang, M. Cao, X.D. Wang, K.Y. Wang, X.H. Xiong, A novel strategy for selective removal and rapid collection of triclosan from aquatic environment using magnetic molecularly imprinted nano-polymers, Chemosphere, 238 (2020) 124640, doi: 10.1016/j.chemosphere.2019.124640.

[2] H.L. So, K.Y. Lin, W. Chu, Triclosan removal by heterogeneous Fenton-like process: studying the kinetics and surface chemistry of Fe_3O_4 as catalyst, J. Environ. Chem. Eng., 7 (2019) 103432, doi: 10.1016/j.jece.2019.103432.

[3] P.R. Teixeira, T.R. Machado, F. Machado, F.F. Sodré, J.G. Silva, B.A.D. Neto, L.G. Paterno, Au nanoparticle-poly(ionic liquid) nanocomposite electrode for the voltammetric detection of triclosan in lake water and toothpaste samples, Microchem. J., 152 (2020) 104421, doi: 10.1016/j.microc.2019.104421.

[4] Y. Lin, X. Jin, G. Owens, Z. Chen, Simultaneous removal of mixed contaminants triclosan and copper by green synthesized bimetallic iron/nickel nanoparticles, Sci. Total Environ., 695 (2019) 133878, doi: 10.1016/j.scitotenv.2019.133878.

[5] J. Lu, Z. Guo, S. Wang, M. Li, N. Wang, L. Zhou, H. Wu, J. Zhang, Remove of triclosan from aqueous solutions by nanoflower MnO_2: insight into the mechanism of oxidation and adsorption, Chem. Eng. J., 426 (2021) 131319, doi: 10.1016/j.cej.2021.131319.

[6] L.A. González-Fernández, N.A. Medellín-Castillo, R. Ocampo-Pérez, H. Hernández-Mendoza, M.S. Berber-Mendoza, C. Aldama-Aguilera, Equilibrium and kinetic modelling of triclosan adsorption on single-walled carbon nanotubes, J. Environ. Chem., 9 (2021) 106382, doi: 10.1016/j.jece.2021.106382.

[7] S.K. Behera, S. Oh, H. Park, Sorption of triclosan onto activated carbon, kaolinite and montmorillonite: effects of pH, ionic strength, and humic acid, J. Hazard. Mater., 179 (2010) 684–691.

[8] M. Triwiswara, C. Lee, J. Moon, S. Park, Adsorption of triclosan from aqueous solution onto char derived from palm kernel shell, Desal. Water Treat., 177 (2020) 71–79.

[9] E.-J. Cho, J.-K. Kang, J.-K. Moon, B.-H. Um, C.-G. Lee, S. Jeong, S.-J. Park, Removal of triclosan from aqueous solution via adsorption by kenaf-derived biochar: its adsorption mechanism study via spectroscopic and experimental approaches, J. Environ. Chem. Eng., 9 (2021) 106343, doi: 10.1016/j.jece.2021.106343.

[10] E. Cho, J. Moon, C. Lee, S. Park, Removal of triclosan from aqueous solution using biochar derived from seed shell of *Aesculus turbinata*, Desal. Water Treat., 266 (2022) 256–267.

[11] J.-K. Kang, E.-J. Seo, C.-G. Lee, J.-K. Moon, S.J. Park, Effectivity and adsorption mechanism of food waste biochar for triclosan removal: a spectroscopic and experimental approach, Biomass Convers. Biorefin., (2021), doi: 10.1007/s13399-021-01997-7.

[12] D. Naghipour, K. Taghavi, M. Ashournia, J. Jaafari, R.A. Movarrekh, A study of Cr(VI) and NH^{4+} adsorption using greensand (glauconite) as a low-cost adsorbent from aqueous solutions, Water Environ. J., 34 (2020) 45–56.

[13] D. Naghipour, L. Hoseinzadeh, K. Taghavi, J. Jaafari, Characterization, kinetic, thermodynamic and isotherm data for diclofenac removal from aqueous solution by activated carbon derived from pine tree, Data Brief, 18 (2018) 1082–1087.

[14] X. Hu, Z. Cheng, Z. Sun, Adsorption of diclofenac and triclosan in aqueous solution by purified multi-walled carbon nanotubes, Pol. J. Environ. Stud., 26 (2017) 87–95.

[15] V. Krstić, T. Urosević, B. Pesovski, A review on adsorbents for treatment of water and wastewaters containing copper ions, Chem. Eng. Sci., 192 (2018) 273–287.

[16] D.P. Mohapatra, D.M. Kirpalani, Advancement in treatment of wastewater: fate of emerging contaminants, Can. J. Chem. Eng., 97 (2019) 2621–2631.

[17] L.F. Cusioli, H.B. Quesada, A.L.B.P. Castro, R.G. Gomes, R. Bergamasco, Development of a new low-cost adsorbent functionalized with iron nanoparticles for removal of metformin from contaminated water, Chemosphere, 247 (2020) 125852, doi: 10.1016/j.chemosphere.2020.125852.
[18] S. Sun, J. Zhu, Z. Zheng, J. Li, M. Gan, Biosynthesis of β-cyclodextrin modified Schwertmannite and the application in heavy metals adsorption, Powder Technol., 342 (2019) 181–192.
[19] S.S. Fiyadh, M.A. Alsaadi, W.Z. Jaafar, M.K. Alomar, S.S. Fayaed, N.S. Mohd, L.S. Hin, A. El-Shafie, Review on heavy metal adsorption processes by carbon nanotube, J. Cleaner Prod., 230 (2019) 783–793.
[20] T. Du, L.-F. Zhou, Q. Zhang, L.-Y. Liu, L. Wen-Bin, H.-K. Liu, Mesoporous structured aluminaosilicate with excellent adsorption performances for water purification, Sustainable Mater.Technol., 18 (2018) e00080, doi: 10.1016/j.susmat.2018.e00080.
[21] N. Eroglu, M. Emekci, C.G. Athanassiou, Applications of natural zeolites on agriculture and food production, J. Sci. Food Agric., 97 (2017) 3487–3499.
[22] N. Rajic, D. Stojakovic, N. Daneu, A. Recnik, The formation of oxide nanoparticles on the surface of natural clinoptilolite, J. Phys. Chem. Solids, 72 (2011) 800–803.
[23] A. Ates, The modification of aluminium content of natural zeolites with different composition, Powder Technol., 344 (2019) 199–207.
[24] N.K.E.M. Khori, T. Hadibarata, M. Elshikh, A.A. Al-Ghamdi, Salmiati, Z. Yusop, Triclosan removal by adsorption using activated carbon derived from waste biomass: isotherms and kinetic studies, J. Chin. Chem. Soc., 65 (2018) 951–959.
[25] S. Lagergren, Zur theorie der sogenannten adsorption gelster stoffe, Kungliga Svenska Vetenskapsakademiens, Handlingar, 24 (1898) 1–39.
[26] Y.S. Ho, G. Mckay, The kinetics of sorption of basic dyes from aqueous solution by sphagnum moss peat, Can. J. Chem. Eng., 76 (1998) 822–827.
[27] C. Lei, Y. Hu, M. He, Adsorption characteristics of triclosan from aqueous solution onto cetylpyridinium bromide (CPB) modified zeolites, Chem. Eng. J., 219 (2013) 361–370.
[28] H.N. Tran, S. You, A. Hosseini-Bandegharaei, H. Chao, Mistakes and inconsistencies regarding adsorption of contaminants from aqueous solutions: a critical review, Water Res., 120 (2017) 88–116.
[29] F.T. Ramos, O.L.S. Weber, E.B. Morais, E.F.G.C. Dores, Z.M. Lima, J.M.P. Novais, Physical, chemical, and microbiological evaluation of a compost conditioned with zeolites, Afr. J. Agric. Res., 13 (2018) 664–672.
[30] Z. Tisler, J. Horacek, J. Safar, R. Velvarska, L. Poliskova, J. Kocik, Y. Gherib, K. Marklova, R. Bulanek, D. Kubicka, Clinoptilolite foams prepared by alkali activation of natural zeolite and their post-synthesis modifications, Microporous Mesoporous Mater., 282 (2019) 169–178.
[31] D. Mantovani, H.B. Quesada, R.S. Antônio, L.F. Cusioli, L. Nishi, A. Diório, P.F. Soares, R. Bergamasco, M.F. Vieira, Adsorption of methylene blue from effluent using golden mussel (*Limnoperna fortunei*) shell as a low-cost material, Desal. Water Treat., 188 (2020) 232–238.
[32] C.S.T. Araújo, V.N. Alves, H.C. Rezende, I.L.S. Almeida, R.M.N. Assunção, C.R.T. Tarley, M.G. Segatelli, N.M.M. Coelho, Characterization and use of *Moringa oleifera* seeds as biosorbent for removing metal ions from aqueous effluents, Water Sci. Technol., 62 (2010) 2198–2203.
[33] H. Kaur, G. Hippargi, G.R. Pophali, A. Bansiwal, Biomimetic lipophilic activated carbon for enhanced removal of triclosan from water, J. Colloid Interface Sci., 535 (2019) 111–121.
[34] J.E. da Silva, F.I.L. Rodrigues, S.N. Pacífico, L.F. Santiago, C.R. Muniz, G.D. Saraiva, R.F. do Nascimento, V. de O. Sousa Neto, Estudo de Cinética e Equilíbrio de Adsorção Empregando a Casca do Coco Modificada Quimicamente para a Remoção de Pb(II) de Banho Sintético, Rev. Virtual Quim., 10 (2018).
[35] M. Triwiswara, C. Lee, J. Moon, S. Park, Adsorption of triclosan from aqueous solution onto char derived from palm kernel shell, Desal. Water Treat., 177 (2020) 71–79.
[36] R.F. Nascimento, A.C.A. Lima, C.B. Vidal, D.Q. Melo, G.S.C. Raulino, Adsorção: aspectos teóricos e aplicações ambientais, Fortaleza, 2020.
[37] V. Vimonses, S. Lei, B. Jin, C.W.K. Chow, C. Saint, Kinetic study and equilibrium isotherm analysis of Congo red adsorption by clay materials, Chem. Eng. J., 148 (2009) 354–364.
[38] G. Blanchard, M. Maunaye, G. Martin, Removal of heavy metals from waters by means of natural zeolites, Water Res., 18 (1984) 1501–1507.
[39] R.M. Karthik, L. Philip, Removal and risk assessment of pharmaceuticals and personal care products in a decentralized greywater treatment system serving an Indian rural community, J. Environ. Chem. Eng., 9 (2021) 106832, doi: 10.1016/j.jece.2021.106832.
[40] I.M. Reck, R.M. Paixão, R. Bergamasco, M.F. Vieira, A.M.S. Vieira, Characterization and use of *Moringa oleifera* seeds as biosorbent for removing metal ions from aqueous effluents, J. Cleaner Prod., 171 (2018) 85–97.
[41] Y. Li, P. Bai, Y. Yan, W. Yan, W. Shi, R. Xu, Removal of Zn^{2+}, Pb^{2+}, Cd^{2+}, and Cu^{2+} from aqueous solution by synthetic clinoptilolite, Microporous Mesoporous Mater., 279 (2019) 203–211.